Chinese Journal of
POLYMER SCIENCE

ARTICLE

https://doi.org/10.1007/s10118-018-2164-1
Chinese J. Polym. Sci. 2018, 36, 1375–1384

Carbon Fibers Decorated by Polyelectrolyte Complexes toward Their Epoxy Resin Composites with High Fire Safety

Xiao-Hui Shi, Li Chen, Bo-Wen Liu, Jia-Wei Long, Ying-Jun Xu, and Yu-Zhong Wang*

School of Chemical Engineering, National Engineering Laboratory of Eco-Friendly Polymeric Materials (Sichuan), State Key Laboratory of Polymer Materials Engineering, Sichuan University, Chengdu 610064, China

Abstract The achievement of both robust fire-safety and mechanical properties is of vital requirement for carbon fiber (CF) composites. To this end, a facile interfacial strategy for fabricating flame-retardant carbon fibers decorated by bio-based polyelectrolyte complexes (PEC) consisting of chitosan (CH) and ammonium polyphosphate (APP) was developed, and its corresponding fire-retarded epoxy resin composites (EP/(PEC@CF)) without any other additional flame retardants were prepared. The decorated CFs were characterized by SEM-EDX, XPS and XRD, indicating that the flame-retardant PEC coating was successfully constructed on the surface of CF. Thanks to the nitrogen- and phosphorous-containing PEC, the resulting composites exhibited excellent flame retardancy as the limiting oxygen index (LOI) increased from 31.0% of EP/CF to 40.5% and UL-94 V-0 rating was achieved with only 8.1 wt% PEC. EP/(PEC8.1@CF) also performed well in cone calorimetry with the decrease of peak-heat release rate (PHRR) and smoke production rate (SPR) by 50.0% and 30.4%, respectively, and the value of fire growth rate (FIGRA) was also reduced to 3.41 $kW \cdot m^{-2} \cdot s^{-1}$ from 4.84 $kW \cdot m^{-2} \cdot s^{-1}$, suggesting a considerably enhanced fire safety. Furthermore, SEM images of the burning residues revealed that the PEC coating exhibited the dominant flame-retardant activity in condensed phase *via* the formation of compact phosphorus-rich char. In addition, the impact strength of the composite was improved, together with no obvious deterioration of flexural properties and glass transition temperature. Taking advantage of the features, the PEC-decorated carbon fibers and the relevant composites fabricated by the cost-effective and facile strategy would bring more chances for widespread applications.

Keywords Fire safety; Carbon fiber composites; Epoxy resin; Polyelectrolyte complexes

Citation: Shi, X. H.; Chen, L.; Liu, B. W.; Long, J. W.; Xu, Y. J.; Wang, Y. Z. Carbon Fibers Decorated by Polyelectrolyte Complexes toward Their Epoxy Resin Composites with High Fire Safety. Chinese J. Polym. Sci. 2018, 36(12), 1375–1384.

INTRODUCTION

Carbon fiber/polymer composites (CFC) have been extensively developed for wide range application of lightweight structures in aerospace, automotive, civil engineering and an increasing number of other consumer and technical applications. Among the different polymer matrices, epoxy resins (EP) have received tremendous attention due to the attractive chemical and thermal resistance, mechanical performance as well as adhesive properties[1–5]. However, EP can be easily ignited and burn vigorously, seriously threatening human lives and property[6–10]. The poor fire resistance often fails to meet safety regulations and hinders their application in many areas, which makes the fire safety of the composite become a challenge and crucial issue.

Some halogen compounds, as high-efficiency flame retardants for EPs and their composites, have been banned considering the harsh requirement on environmental friendliness and human's health[11–13]. In this context, halogen-free flame retardants are currently being exploited, and phosphorus-containing flame retardants have sprang up in both academia and industrial circles[14–19]. Among them, intumescent flame retardants (IFRs) are one type of the most competitive flame retardants for EPs and their composites[20–22]. We reported a series of modified ammonium polyphosphate (APP) as intumescent flame-retardant curing agent for EP and desired flame retardancy was obtained[22–24]. Li *et al.*[25] incorporated multiwall carbon nanotubes doped polyethersulfone film (PES-MWCNT) in CF-reinforced epoxy composites to improve the flame retardancy of the composite but limited improvement was achieved. Rajaei *et al.*[8] used APP and talc as flame retardants and improved the flame retardancy of epoxy, but the strengths were compromised due to the incompatibility of the additives with epoxy. In general, imperfections like inefficiency or poor mechanical properties are still inevitable for the method of directly incorporating flame retardants into EP matrix.

In order to address the above issues, we tried modifying the fibers firstly, and then used the modified fibers to prepare flame-retard composites. Herein, the decorated carbon fibers were fabricated using a novel strategy through simply soaking CF into a solution of polyelectrolyte mixture

* Corresponding author: E-mail yzwang@scu.edu.cn

Received May 18, 2018; Accepted May 28, 2018; Published online July 4, 2018

© Chinese Chemical Society
Institute of Chemistry, Chinese Academy of Sciences
Springer-Verlag GmbH Germany, part of Springer Nature 2018

consisting of chitosan (CH) and APP. CH, a potential and promising green charring agent, can act as a carbon source, and APP can act as an acid source, reacting with the EP matrix to form an intumescent char[26–30]. The strategy focused on the facile and quick construction of IFR-decorated coatings onto CF to improve the flame retardancy of EP/CF without addition of other flame retardants, which was easy to operate and the decoration process was completed under mild conditions (*e.g.*, room temperature, atmospheric pressure and using water as solvent) in a few minutes. The decorated coating content on CFs was tunable so that desired flame retardancy and satisfactory mechanical properties of the composites could be obtained. The decorated CF was characterized thoroughly, and the flame retardancy, burning behavior and mechanical properties of the resulting composites were investigated.

EXPERIMENTAL

Materials

Unidirectional T700 12K carbon fibers (CFs) with 200 g·m^{-2} of area density were produced by Toray Industrial Co. Ltd., (Japan). Diglycidyl ether of biphenol A-type (DGEBA E-51) was purchased from Xingchen Synthetic Material Co. Ltd., (Nantong, China). 4,4′-Diaminodiphenyl sulfone (DDS, 98%) was commercially supplied by Sinopharm Chemical Reagent Co., Ltd. (Shanghai, China). Commercial APP (form II) was manufactured by Taifeng Fire Retardants Co., Ltd. (Sichuan, China) and used as received. Chitosan (CH, $M_w \approx 10$ kDa, deacetylated ≥ 85%) was purchased from Jinan Haidebei Marine Bioengineering Co., Ltd, China.

Surface Decoration of Carbon Fibers with Polyelectrolyte Complexes

The aqueous solution coating on CFs mainly consisted of polyelectrolyte complexes (PEC) formed between oppositely charged CH and APP[31–33] based on the ionic exchange reaction. Afterwards, PEC coating was constructed on CF surface by a facile soaking method as follows: the aqueous solutions with different concentrations of CH and APP were firstly poured into the coating basin with a certain dimension and amount of CFs. Then CFs were soaked in the mixture solution for certain time and dried in an oven at 80 °C. Finally, the decorated CFs were dried under vacuum at 80 °C for 12 h to obtain PEC@CF.

Preparation of Carbon Fiber Reinforced Composites

In this work, all composites were fabricated by hand lay-up technique followed by compression moulding. Firstly, the mold with a thin layer of release agent and a certain dimension of CFs were preheated at 90 °C. Then epoxy resin (DGEBA E-51) was placed in a glass flask and heated at 125 °C under stirring in an oil bath, and the required amount of DDS was added and dispersed under a constant temperature of 125 °C until the mixture became uniform and transparent to saturate CF or PEC@CF. Subsequently, the saturated CFs or PEC@CF were unidirectionally placed into the preheated mold and degassed in a vacuum oven at 80 °C for at least 30 min until no bubble emerged. Thereafter, the mold was transformed into a vulcanizing machine and the EP composites were cured as the following procedure: 130 °C/2 h and 200 °C/2 h with a pressure of 1 MPa for the last 3.5 h. The pristine CF and PEC@CF reinforced EP composites were named as EP/CF and EP/(PEC@CF), respectively.

Characterizations

Surfacial morphology, elemental composition and distribution, and burning residue of PEC@CF were characterized by scanning electronic microscopy (SEM, PHOX, Phenom word) together with energy dispersive X-ray spectrometry (EDX). 3D roughness of PEC@CF was also observed by Phenom ProX at the mode of 3D Roughness Reconstruction. All the samples were coated with gold before SEM observation.

Element composition and chemical states of PEC@CF were assessed by X-ray photoelectron spectroscopy (XPS, XSAM80 Kratos Co, UK) using Al Kα excitation radiation ($h\nu$ = 1486.6 eV).

Fourier transform infrared spectroscopy (FTIR) was performed on a Nicolet 6700 spectrometer with attenuated total reflection (ATR) of Spectra-Tech Foundation Endurance using 32 scans in the frequency region of 4000−400 cm^{-1}.

The X-ray diffraction (XRD) patterns using Cu Kα radiation (λ = 1.542 Å) were recorded with a power DX-1000 diffractometer (Dandong Fangyuan, China) at the scanning rate of 0.02 (°)·s^{-1} in the range of 10°–70°. The XRD data were collected in reflection mode.

The thermal stability of the testing samples under inert or oxidative atmosphere was investigated by thermogravimetry analysis (TGA) 209 F1 (NETZSCH, Germany). The samples were heated from 40 °C to 700 °C at a rate of 10 °C·min^{-1} under nitrogen or air flow of 50 mL·min^{-1}.

The flame retardancy of the composites was evaluated by limiting oxygen index (LOI, HC-2C, Jiangning, China) and Underwriter Laboratory 94 vertical burning test (UL-94 V, CZF-2, Jiangning, China) according to ASTM D2863-10 and ATSM D3801-10, respectively. The burning behavior of the samples was investigated by cone calorimetry (Fire Testing Technology, UK). The samples with dimension of 100 mm × 100 mm × 3.2 mm were exposed to a radiant cone at a heat flux of 50 kW·m^{-2} according to ISO 5660. All samples were mounted by frame with aluminum foil backing.

Raman spectra were recorded with inVia Laser Raman Spectrometer (HORIBA Jobin Yvon Co., Ltd., France) at room temperature with an excitation wavelength of 532.17 nm and wavenumber from 800 cm^{-1} to 2000 cm^{-1}.

The Izod notched impact strength, three-point short beam flexural strength and apparent interlaminar shear strength were tested according to GB/T 1843-2008 (plastics-determination of Izod impact strength), GB/T 3356-2014 (test method for flexural properties of orientational fiber reinforced polymer matrix composite materials) and JC/T 773-2010 (fiber-reinforced plastics composites-determination of apparent interlaminar shear strength by short-beam method) with rectangular specimens of 80 mm × 10 mm × 2 mm, 100 mm × 10 mm × 2 mm and 20 mm × 10 mm × 2 mm, respectively by using a universal testing

machine (MTS SYSTEMS CO., LTD, China).

Dynamic mechanical analysis (DMA Q800, TA instruments) was performed in a three point bending model (constant frequency = 1.0 Hz, oscillation amplitude = 10.0 μm and heating rate = 5 °C·min^{-1}). The samples were tested with a size of 40 mm × 10 mm × 2 mm.

RESULTS AND DISCUSSION

Characterization of PEC@CF

The surface morphologies of pristine CF and PEC@CF were imaged by SEM and the results are shown in Fig. 1. The numbers 5.2, 6.9 and 8.1 were the weight contents of PEC in their composites. Obvious differences could be found for the morphology between pristine CF and PEC@CF. The pristine CF had a clean and smooth surface, and the boundaries of each CF were distinct. But for PEC@CF, the boundaries became vague, and gaps between each CF were gradually filled with PEC due to the attachment of the decorated coating on CFs. Moreover, the different morphologies of the decorated CF with well-distributed but bad-dispersed decorated coatings were observed as illustrated in Figs. 1(b1)–1(d1), which was attributed to the fast self-assembling and deposition rate of PEC as a consequence of the high molecular weight of CH, leading to a slight aggregation and adsorption of APP when deposited on CFs. On the other hand, the increased concentration of APP resulted in larger viscosity and higher deposition rate of PEC, which accelerated PEC self-assembling and further adsorption of the unreacted APP particles, displaying the different morphologies of the decorated CFs. This indicated the controllability of the PEC coating by tuning the concentration collocation of polyelectrolytes. In addition, the different morphologies were exhibited visually by 3D images as illustrated in Figs. 1(a2)–1(d2). The obvious discrepancy in morphology and surface roughness of CFs played a key role in the final mechanical properties of the composites. These morphologies explicitly evidenced that PEC-decorated CFs were successfully obtained by simple soaking process.

In order to obtain the information concerning the element composition and elemental chemical states of PEC@CF, SEM-EDX and XPS were performed and the results are presented in Fig. 2. XPS and EDX spectra clearly revealed that nitrogen (N) and phosphorus (P) elements were only detected in PEC@CF compared with the pristine CF and each detected element had a good distribution in PEC as illustrated in Figs. 2(a)–2(d). Notably, in addition to the peaks at 401.3 and 398.9 eV attributed to $-NH_4^+$ and C—N bonds in the fitting curves of N1s, a new binding energy peak at 399.6 eV appeared as shown in Fig. 2(e). It was assigned to $-NH_3^+$ derived from PEC, indicating the occurrence of ion exchange reaction between CH and APP during decorated process. This was further evidenced by the FTIR spectra (Fig. 2f) as the new peak at 1535 cm^{-1} appeared[24, 34], verifying the stability of PEC that ensured a positive effect on the subsequent properties of the composite. The decorated CF was further investigated by XRD and the representative peaks of CF ($2\theta \approx$ *ca.* 25.3° and 43.5°)[35] appeared in the XRD pattern (Fig. 2g) of PEC@CF coupled with the characteristic peaks corresponding to PEC, indicating the successful construction of PEC on CF but without destruction of the crystallized graphitic basal planes of CF for this coating method. According to these results, it was confirmed that PEC decorated CF was successfully fabricated by the facial soaking strategy and some active groups were introduced onto CF surface, which had potential positive influence on the mechanical properties of the resulting composites.

Thermal Stability

Thermogravimetric analysis (TGA) was utilized to investigate the thermal stability of the composites under both N_2 and air atmospheres, and the weight loss and derivative weight curves are shown in Fig. 3. The corresponding data are summarized in Table 1. All composites exhibited a one-

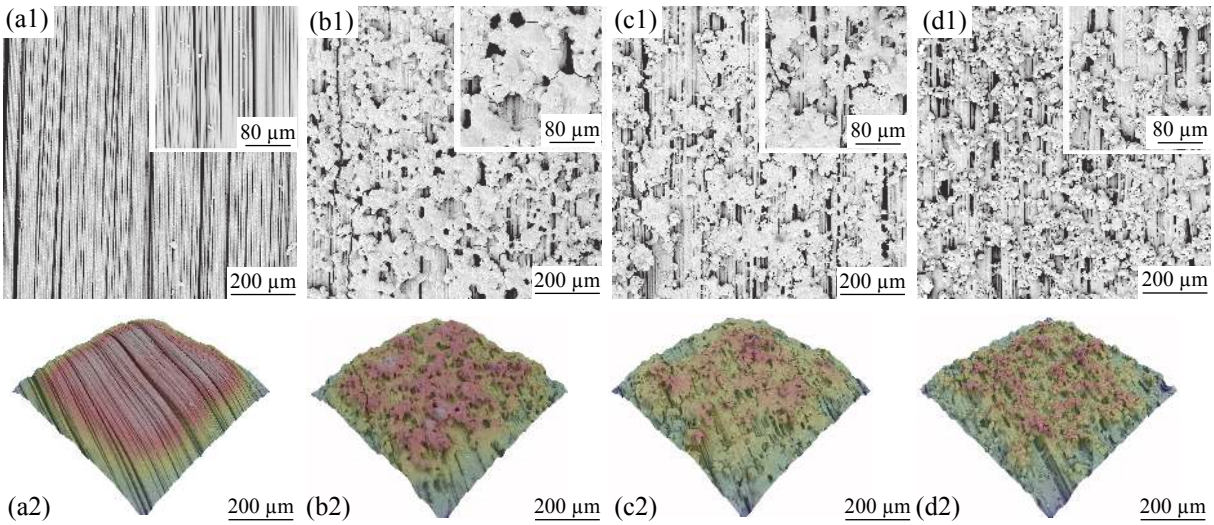

Fig. 1 SEM images at different magnifications and the corresponding 3D morphologies of (a1, a2) pristine CF, (b1, b2) PEC5.2@CF, (c1, c2) PEC6.9@CF, and (d1, d2) PEC8.1@CF (subscript 1 represents the SEM images, subscript 2 denotes the 3D morphologies.)

https://doi.org/10.1007/s10118-018-2164-1

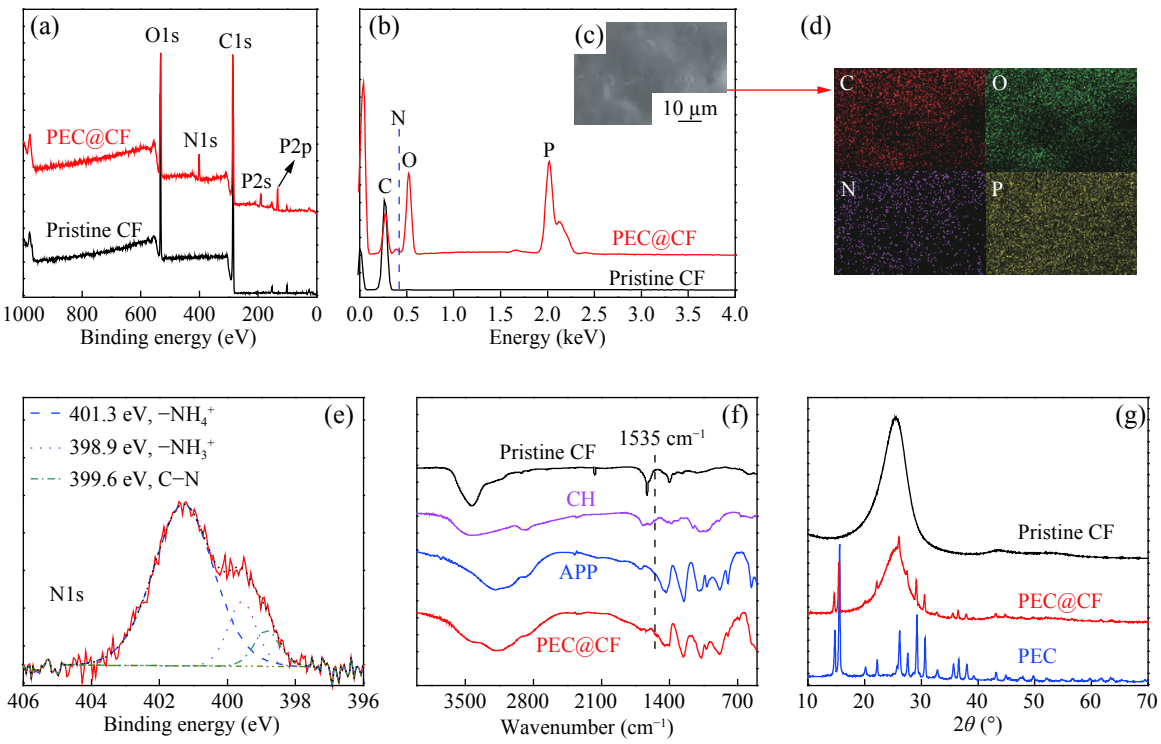

Fig. 2 (a) XPS full survey spectra of pristine CF and PEC@CF; (b) EDX spectra of pristine CF and PEC@CF; (d) Corresponding EDX elements mapping images of the imbedded SEM morphology (c); (e) XPS N1s spectra of PEC@CF; (f) FTIR spectra of CH, APP, pristine CF and PEC@CF; (g) X-ray diffraction patterns of PEC, pristine CF and PEC@CF

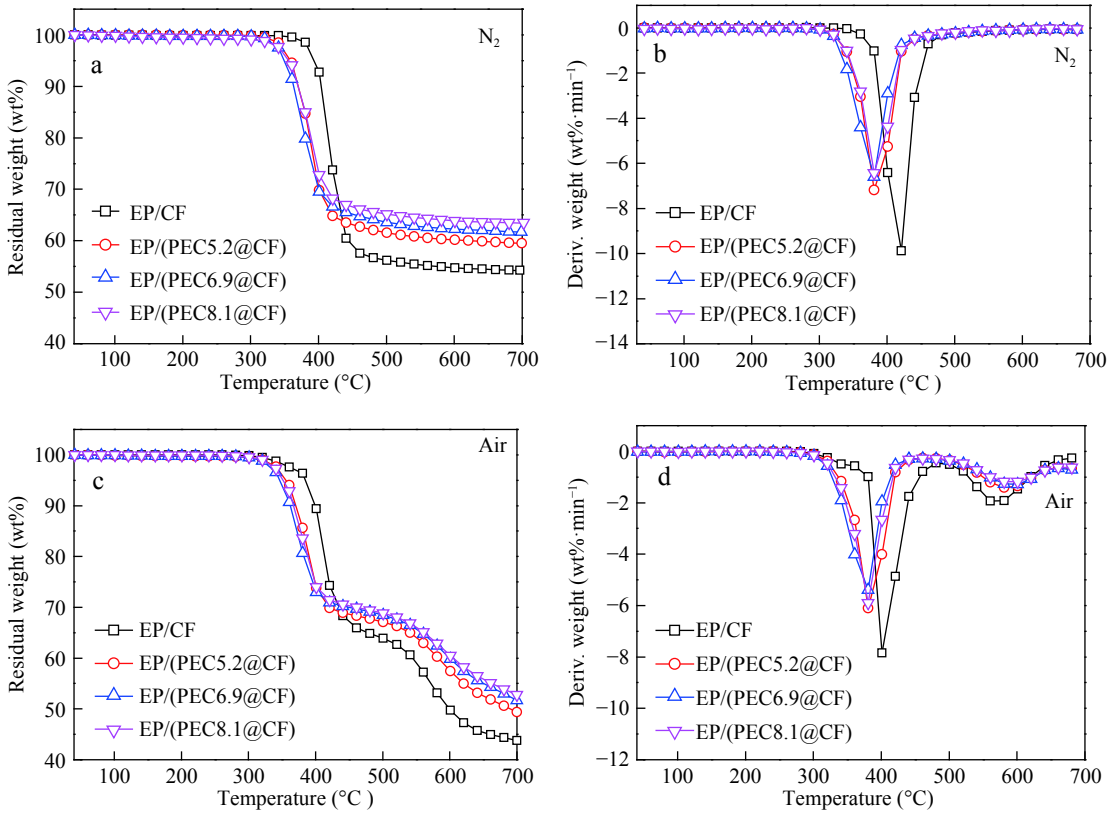

Fig. 3 (a, c) TG and (b, d) DTG curves of EP/CF and EP/(PEC@CF) composites at a heating rate of 10 °C·min^{-1} under (a, b) N_2 and (c, d) air atmospheres

step degradation process in N_2 atmosphere as presented in Fig. 3(a), which was mainly attributed to the depolymerization of C—O—C and C—N—C in EP matrix. However, owing to the preceeding decomposition of PEC

Table 1 Thermogravimetric properties of EP/CF and EP/(PEC@CF) composites

Sample	N_2			Air			
	$T_{5\%}$ [a] (°C)	T_{max1} [b] (°C)	R_{700} [c] (wt%)	$T_{5\%}$ (°C)	T_{max1} (°C)	T_{max2} (°C)	R_{700} [c] (wt%)
EP/CF	397	416	54.1	390	406	571	43.8
EP/(PEC5.2@CF)	337	369	62.5	336	368	603	52.6
EP/(PEC6.9@CF)	337	370	63.6	337	370	612	53.6
EP/(PEC8.1@CF)	338	369	64.6	336	370	614	54.8

[a] The temperature where 5 wt% of weight was lost; [b] The temperature where the maximum weight loss occurred; [c] The residual weight at 700 °C

coating, the initial degradation temperature (defined as the temperature at which 5 wt% of weight loss, $T_{5\%}$) and T_{max} were all considerably decreased relative to those of EP/CF. Then the weight loss rate under heating was suppressed, resulting in the enhanced residual weight (from 54.1 wt% to the highest of 64.6 wt%) at higher temperatures. As a contrast, the degradation in air atmosphere of composites displayed a two-step weight loss due to the participation of oxygen—the first weight-losing step was induced by the decomposition of macromolecular networks and the second was attributed to the further oxidation of the char layer. Similar to the degradation in N_2 atmosphere, $T_{5\%}$ and T_{max1} of the flame-retardant composites decreased considerably. These phenomena were ascribed to the preceeding decomposition of PEC flame-retardant coatings, *in situ* generation of some reactive acid such as phosphoric and poly-/pyro-/ultra-phosphoric acids, which were able to catalyze and accelerate the degradation of EP matrix to form a relatively thermally stable char structure containing polyphosphates under 300–450 °C. Then the obtained residual chars could be further oxidized, carbonized and even broken due to the presence of oxygen around 500–700 °C. On the other hard, a higher degradation temperature of EP/(PEC@CF) was also observed thanks to the improved thermal stability of residues, which was capable of limiting and even blocking off the transfer of energy to the underlying combustible substrate, resulting in the decreased weight loss rate and the increased burning residue of EP/(PEC@CF) at 700 °C. All above results indicated that PEC coating exhibited potential to achieve better flame retardancy by the higher char yield and the lower degradation rate.

Flame Retardancy and Burning Behaviors

In order to assess the flame retardancy of composites EP/CF and EP/(PEC@CF), LOI and UL-94 V, two typical small-scale tests to characterize the flammability of plastic materials, were carried out, and the results are listed in Table 2. PEC could effectively increase the LOI value from 31.0% of EP/CF to 36.0% of composite with 5.2 wt% PEC as listed in Table 2. The LOI value of the composite was further elevated to 40.5% and the UL-94 V rating was upgraded to V-0 rating when 8.1 wt% of PEC was introduced to the composite, indicating that PEC performed high flame-retardant efficiency in EP/CF composite. Additionally, cone calorimetry was employed to evaluate the influence of PEC coatings on burning behaviors of EP/CF under a realistic fire scenario and the characteristic curves are shown in Figs. 4 and 5, and the related data are collected in Table 3.

In cone calorimetric test, the fire was fully developed when EP/CF was ignited with a high PHRR of 508.3 $kW\cdot m^{-2}$ and terminated within short time of 300 s with a higher THR of 47.8 $MJ\cdot m^{-2}$. In contrast, PEC remarkably changed the burning behavior of EP/CF. Initially, EP/(PEC@CF) was ignited a little earlier due to the preceeding decomposition of PEC at the beginning of combustion, in consistent with the TG results. Secondly, EP/(PEC@CF) showed a distinctly decreased PHRR of 255.9 $kW\cdot m^{-2}$ by 50.0% with an introduction of 8.1 wt% PEC, resulting in a reduced THR relative to that of EP/CF. Based on the HRR data, the fire growth rate (FIGRA, defined as the ratio of PHRR to the time when it was achieved, TTPHRR) had been calculated to assess the fire hazard (burning propensity) of the composites. For EP/CF, the value of FIGRA was 4.84 $kW\cdot m^{-2}\cdot s^{-1}$. However, the FIGRA value of EP/(PEC8.1@CF) was reduced to 3.41 $kW\cdot m^{-2}\cdot s^{-1}$. Generally, a lower FIGRA value indicates that the time to flashover is delayed, which means that there is enough time to evacuate people in distress and/or reach for the fire extinguishers. In addition, during fire, the high yields of smoke, asphyxiant and toxic gases are held responsible for most of the deaths through inhalation. Herein, as illustrated in Fig. 5, both the smoke production rate (SPR) and the total smoke production (TSP) of EP/(PEC8.1@CF) also decreased by 30.4% and 30.7%, respectively, with comparison to those of EP/CF, indicating that the introduction of PEC coating on CF surface enhanced the fire safety of the composites.

To fully elucidate the effects of PEC on EP/(PEC@CF), SEM was applied to observe the morphologies of burning residues and the relevant results are summarized in Fig. 6. For EP/CF, a little amount of loose char with obvious holes and cracks attached on CFs and the gaps of the residual CF were exposed with traces of char as the EP matrix was nearly burnt out (Figs. 6a1 and Figs. 6a2). However, for EP/(PEC@CF), the visibly increased residual char without

Table 2 Formulation and flame retardancy for EP/CF and EP/(PEC@CF)

Sample	Weight content		LOI (%)	UL-94 V		
	CF (wt%)	PEC (wt%)		t_1 (s)	t_2 (s)	Rating
EP/CF	47.5	–	31.0 ± 0.5	0	> 30	No rating
EP/(PEC5.2@CF)	46.5	5.2	36.0 ± 0.5	0	> 30	No rating
EP/(PEC6.9@CF)	45.9	6.9	38.5 ± 0.5	0	11 ± 8	V-1
EP/(PEC8.1@CF)	45.2	8.1	40.5 ± 0.5	0	0	V-0

https://doi.org/10.1007/s10118-018-2164-1

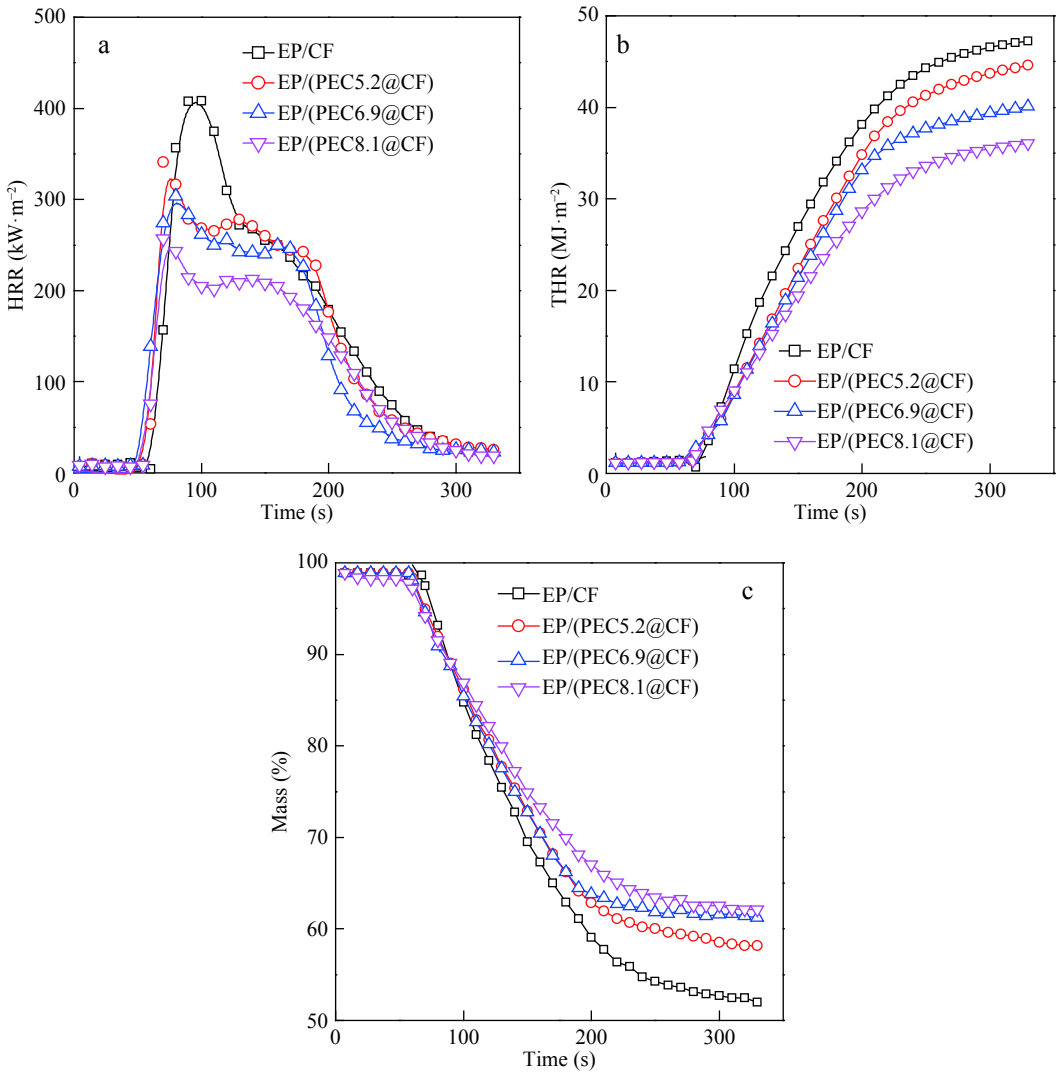

Fig. 4 The characteristic curves of (a) heat release rate (HRR), (b) total heat release (THR), and (c) burning residue percentage for EP/CF and EP/(PEC@CF) recorded from cone calorimetry

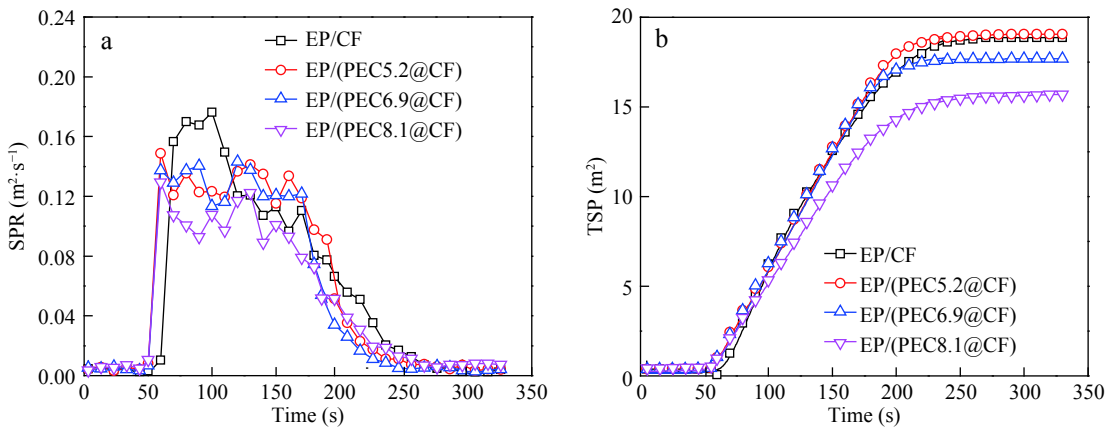

Fig. 5 The (a) smoke production rate (SPR) and (b) total smoke production (TSP) for EP/CF and EP/(PEC@CF) recorded from cone calorimetry

obvious cracks and fissures were observed and became gradually compact with further introduction of PEC as shown in Figs. 6(b2)–6(d2). Meanwhile, the char increasingly filled up the interspaces of each individual CF and combined CFs together as presented in Figs. 6(b1)–6(d1), forming a perfect shield to prevent the underlying materials from the fire. The detected S and P elements in burning residues (Figs. 6e1 and 6e2) suggested that EP was

Table 3 The related data for EP/CF and EP/(PEC@CF) obtained from cone calorimetry at 50 kW·m^{-2}

Sample	TTI [a] (s)	THR (MJ·m^{-2})	PHRR [b] (kW·m^{-2})	TTPHRR [c] (s)	FIGRA (kW·m^{-2}·s^{-1})	TSR (m^2·m^{-2})	TSP (m^2)	Residue (wt%)
EP/CF	54	47.8	508.3	105	4.84	2540.2	22.5	51.7
EP/(PEC5.2@CF)	51	44.0	358.0	75	4.78	2155.3	19.0	58.5
EP/(PEC6.9@CF)	50	39.6	307.5	80	3.84	2000.1	17.7	61.6
EP/(PEC8.1@CF)	49	35.5	255.9	75	3.41	1768.5	15.6	62.6

[a] TTI was time to ignition; [b] PHRR was peak of heat release rate; [c] TTPHRR was the time to PHRR

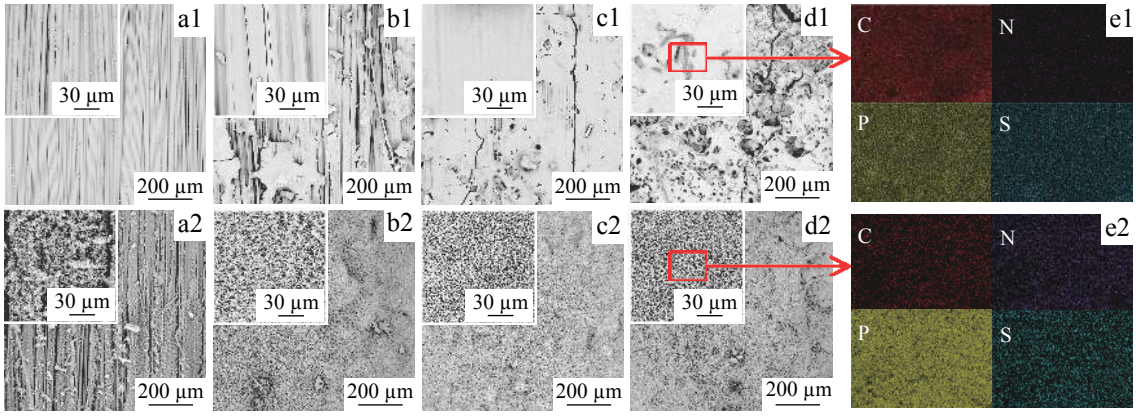

Fig. 6 SEM images of (a1–e1) inner surface and (a2–e2) outside surface of burning residues for (a1, a2) EP/CF, (b1, b2) EP/(PEC5.2@CF), (c1, c2) EP/(PEC6.9@CF), and (d1, d2) EP/(PEC8.1@CF) obtained after cone calorimetry test; (e1, e2) The corresponding EDX elements mapping images of EP/(PEC8.1@CF) (Oxygen was also detected but not presented.)

not burnt out in EP/(PEC@CF) due to the PEC decoration on CF's surface, indicating an obvious flame-retardant activity in the condensed phase. In addition, the good distribution of each element in the burning residues was also beneficial to improve the flame retardancy of the composites.

Based on the aforementioned results, PEC flame-retardant coatings would decompose at relatively low temperatures as discussed in TGA, and the CH moieties as carbon source would be charred first under the catalytic effect of phosphoric acid and poly-/ultra-/pyro-derivatives generated from the preceeding decomposition of APP moieties. The produced phosphate compounds concentrated on CFs would also catalyze and facilitate the adjacent EP to dehydrate and carbonize to form the phosphorus-rich aromatization structures, which would grow along with CF, thus a fire protecting shield consisting of non-flammable and high-strength CF as framework and P-containing condensed char as stuffing was obtained. The special shield could isolate the transfer of oxygen, heat and the combustible volatiles feeding back into the burning zone, and then protected the unburned materials, showing a typical flame-retardant effect in condensed phase.

Mechanical Properties and Dynamic Mechanical Behaviors

The mechanical properties including impact strength, flexural strength and interlaminar shear strength (ILSS) of the composites were also tested systematically and the results are shown in Fig. 7. The impact strength of EP/(PEC@CF) had varying degrees of increment relative to that of EP/CF, and EP/(PEC8.1@CF) had the maximum impact resistance with an increase of 26.4% as presented in Fig. 7. The increment could be explained by "fiber-bridging effect"[36, 37]. When the cracks propagated in EP matrix and reached interface, a few matrix cracks would deflect to interface rather than penetrate the fibers due to the soft nature of PEC, which was also demonstrated by the fracture surfaces as shown in Fig. 8. Some micro-cracks and delamination between fibers and matrix were observed, which could capture and efficiently consume the fracture energy, resulting in the enhanced impact resistance but decreased ILSS[38, 39]. Nevertheless, the flexural strength decreased a little from 977.2 MPa to 863.6 MPa for EP/(PEC8.1@CF), which was attributed to the improved compatibility caused by the polar groups like —OH, —NH— and —P—O— derived from PEC and the strong mechanical interlocking between CFs and EP matrix due to the increased roughness of the decorated CFs (Figs. 1a1–1d2) that compensated the strength. Moreover, it was noticeable that flexural modulus of EP/(PEC@CF) was unaffected by PEC coating because the decorated strategy employed in this study did not etch CFs and introduce defects or damages on CFs surface, maintaining the fundamental graphitic structures and strength of CF.

The mechanical properties of composites under dynamic load and temperature were characterized by DMA, which could provide valuable insights into the actual application environment of composites. The variations of the storage modulus and the tanδ as a function of temperature for composites are shown in Fig. 9. EP/(PEC@CF) composites could still maintain the stiffness of EP/CF at higher temperature below T_g (the temperature of the maximum tanδ), suggesting that PEC coating had negligible effect on the stiffness of the composite. EP/CF showed a T_g at 229 °C and it had a mild decrease of 21 °C for EP/(PEC5.2@CF),

https://doi.org/10.1007/s10118-018-2164-1

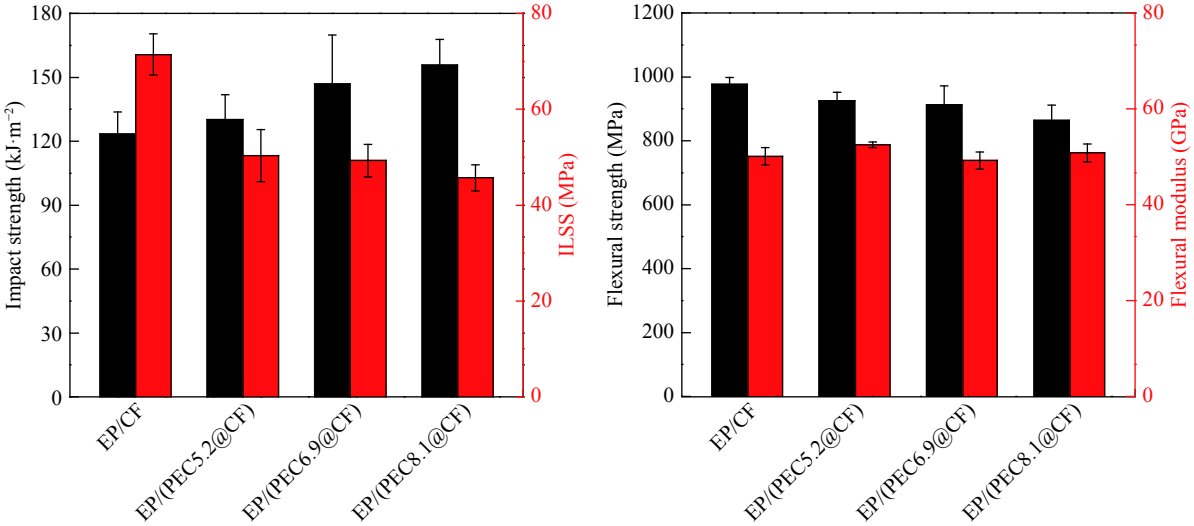

Fig. 7 Mechanical properties of EP/CF and EP/(PEC@CF)

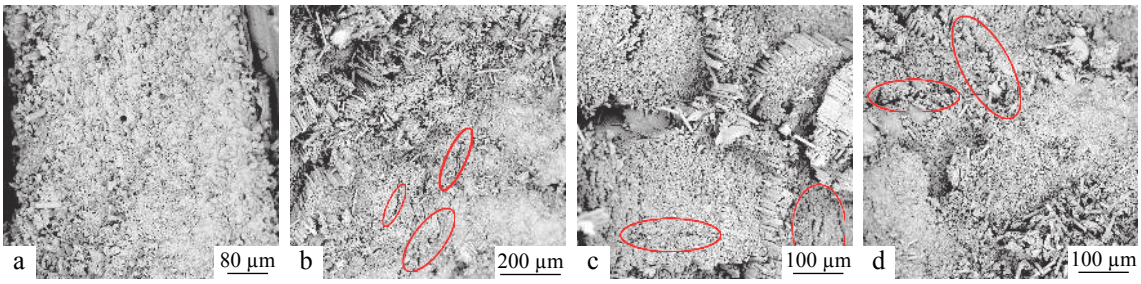

Fig. 8 The fractured surfaces after impact strength test of (a) EP/CF, (b) EP/(PEC5.2@CF), (c) EP/(PEC6.9@CF), and (d) EP/(PEC8.1@CF)

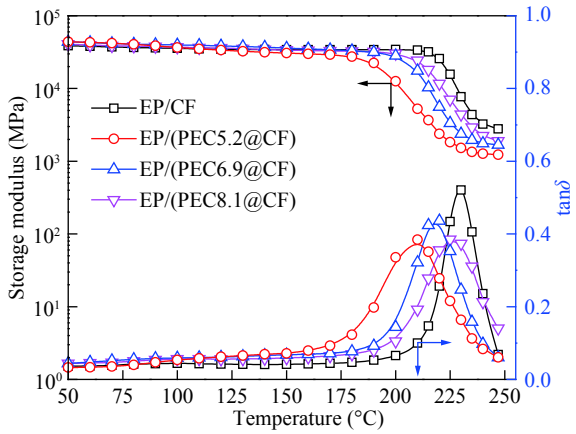

Fig. 9 DMA curves of the composites EP/CF and EP/(PEC@CF)

then steadily improved to 218 and 226 °C with further incorporation of PEC. The reversion of T_g was mainly determined by the balance between the confinement effect and the influence of curing reaction resulting from PEC coating. The presence of PEC coating containing some APP particles caused the under-curing of the EP matrix, while it also acted as the barriers to restrict the mobility of chain segments[40, 41], and it was pronounced that the confinement effect became dominant gradually with the increased loading of PEC, resulting in an insignificant reduction of T_g for EP/(PEC8.1@CF) with respect to that of EP/CF. Specially, the decreased but widened tanδ peak might be related to the restrained chain mobility and the enhanced interface friction between matrix and CF[42–44].

CONCLUSIONS

In this work, a novel strategy for fabricating fire-retardant carbon fiber reinforced epoxy resin composites was developed. The carbon fibers were decorated *via* a facile soaking in polyelectrolyte complexes consisting of flame-retardant polyanion (APP) and bio-based polycation (CH) and the decorated carbon fibers were used to reinforce epoxy resin composites, which displayed high fire safety. CH/APP coating exerted flame retardancy in condensed phase, by which phosphoric acid and its poly-/ultra-/pyro-derivatives generated from the preceeding decomposition of PEC dehydrated and carbonized EP matrix, obtaining the burning residue composed of non-flammable and high-strength CFs as framework and P-containing condensed char as stuffing that exhibited excellent flame retardancy. Consequently, EP/(PEC8.1@CF) possessed the LOI value of 40.5% and achieved V-0 rating easily in the UL-94 V test. EP/(PEC8.1@CF) performed a great amelioration in cone calorimetry with the decreased PHRR and SPR by 50.0%

and 30.4%, respectively, and considerably enhanced fire safety with the reduction of the FIGRA value from 4.84 $kW \cdot m^{-2} \cdot s^{-1}$ to 3.41 $kW \cdot m^{-2} \cdot s^{-1}$. Furthermore, EP/(PEC@CF) exhibited desirable mechanical properties and almost unchanged T_g. The distinctive PEC-decorated carbon fiber made it ideal for fabricating carbon fiber-reinforced composite for mass production as it permitted the compatibility and feasibility on industrial application. In all case, the facile and cost-effective strategy employed in this study has potential to fabricate EP/CF composite with satisfactory flame retardancy and mechanical properties.

ACKNOWLEDGMENTS

Financial supports by the National Natural Science Foundation of China (Nos. 51773137 and 51721091) and the Sichuan Province Youth Science and Technology Innovation Team (No. 2017TD0006) are sincerely acknowledged. The authors would also like to thank the Analysis and Testing Center of Sichuan University for the XPS measurements.

REFERENCES

1 Yang, X. L.; Li, K.; Xu, M. Z.; Liu, X. B. Designing a phthalonitrile/benzoxazine blend for the advanced GFRP composite materials. Chinese J. Polym. Sci. 2017, 36(1), 106−112.
2 Nunna, S.; Creighton, C.; Fox, B. L.; Naebe, M.; Maghe, M.; Tobin, M. J.; Bambery, K.; Vongsvivut, J.; Hameed, N. The effect of thermally induced chemical transformations on the structure and properties of carbon fibre precursors. J. Mater. Chem. A 2017, 5(16), 7372−7382.
3 Xu, Y. J.; Wang, J.; Tan, Y.; Qi, M.; Chen, L.; Wang, Y. Z. A novel and feasible approach for one-pack flame-retardant epoxy resin with long pot life and fast curing. Chem. Eng. J. 2018, 337, 30−39.
4 Shen, D.; Xu, Y. J.; Long, J. W.; Shi, X. H.; Chen, L.; Wang, Y. Z. Epoxy resin flame-retarded via a novel melamine-organophosphinic acid salt: thermal stability, flame retardancy and pyrolysis behavior. J. Anal. Appl. Pyrolysis 2017, 128, 54−63.
5 Li, W. W.; Kang, H. L.; Xu, J.; Liu, R. G. Effects of ultra-high temperature treatment on the microstructure of carbon fibers. Chinese J. Polym. Sci. 2017, 35(6), 764−772.
6 Xu, M. J.; Xia, S. Y.; Liu, C.; Li, B. Preparation of poly(phosphoric acid piperazine) and its application as an effective flame retardant for epoxy resin. Chinese J. Polym. Sci. 2018, 36(5), 655−664.
7 Liao, D. J.; Xu, Q. K.; McCabe, R. W.; Babu, H. V.; Hu, X. P.; Pan, N.; Wang, D. Y.; Hull, T. R. Ferrocene-based nonphosphorus copolymer: synthesis, high-charring mechanism, and its application in fire retardant epoxy resin. Ind. Eng. Chem. Res. 2017, 56(44), 12630−12643.
8 Rajaei, M.; Wang, D. Y.; Bhattacharyya, D. Combined effects of ammonium polyphosphate and talc on the fire and mechanical properties of epoxy/glass fabric composites. Ind. Eng. Chem. Res. 2017, 113, 381−390.
9 Xu, Y. J.; Chen, L.; Rao, W. H.; Qi, M.; Guo, D. M.; Liao, W.; Wang, Y. Z. Latent curing epoxy system with excellent thermal stability, flame retardancy and dielectric property. Chem. Eng. J. 2018, 347, 223−232.
10 Agrawal, S.; Narula, A. K. Synthesis, characterization of phosphorus containing diamide-diimide-tetraamines based on L-tryptophan amino acid and their effect on flame retardancy of epoxy resins. Chinese J. Polym. Sci. 2014, 32(2), 197−208.
11 Aschberger, K.; Campia, I.; Pesudo, L. Q.; Radovnikovic, A.; Reina, V. Chemical alternatives assessment of different flame retardants-A case study including multi-walled carbon nanotubes as synergist. Environ. Int. 2017, 101, 27−45.
12 Curran, I. H.; Liston, V.; Nunnikhoven, A.; Caldwell, D.; Scuby, M. J.; Pantazopoulos, P.; Rawn, D. F.; Coady, L.; Armstrong, C.; Lefebvre, D. E. Toxicologic effects of 28-day dietary exposure to the flame retardant 1,2-dibromo-4-(1,2-dibromoethyl)-cyclohexane (TBECH) in F344 Rats. Toxicology 2017, 377, 1−13.
13 Liao, S. F.; Deng, C.; Huang, S. C.; Cao, J. Y.; Wang, Y. Z. An efficient halogen-free flame retardant for polyethylene: piperazinemodified ammonium polyphosphates with different structures. Chinese J. Polym. Sci. 2016, 34(11), 1339−1353.
14 Jian, R.; Wang, P.; Duan, W.; Wang, J.; Zheng, X.; Weng, J. Synthesis of a novel P/N/S-containing flame retardant and its application in epoxy resin: thermal property, flame retardance, and pyrolysis behavior. Ind. Eng. Chem. Res. 2016, 55(44), 11520−11527.
15 Rao, W. H.; Xu, H. X.; Xu, Y. J.; Qi, M.; Liao, W.; Xu, S.; Wang, Y. Z. Persistently flame-retardant flexible polyurethane foams by a novel phosphorus-containing polyol. Chem. Eng. J. 2018, 343, 198−206.
16 Sun, J.; Yu, Z.; Wang, X.; Wu, D. Synthesis and performance of cyclomatrix polyphosphazene derived from trispiro-cyclotriphosphazene as a halogen-free nonflammable material. ACS Sustain. Chem. Eng. 2013, 2(2), 231−238.
17 Wang, W.; Wen, P.; Zhan, J.; Hong, N.; Cai, W.; Gui, Z.; Hu, Y. Synthesis of a novel charring agent containing pentaerythritol and triazine structure and its intumescent flame retardant performance for polypropylene. Polym. Degrad. Stab. 2017, 144, 454−463.
18 Wang, X.; Zhou, S.; Guo, W. W.; Wang, P. L.; Xing, W.; Song, L.; Hu, Y. Renewable cardanol-based phosphate as a flame retardant toughening agent for epoxy resins. ACS Sustain. Chem. Eng. 2017, 5(4), 3409−3416.
19 Du S. L.; Lin X. B.; Jian, R. K.; Deng C.; Wang Y. Z. Flame-retardant wrapped ramie fibers towards suppressing "candlewick effect" of polypropylene/ramie fiber composites. Chinese J. Polym. Sci. 2015, 33(1), 84−94.
20 Tai, Q.; Hu, Y.; Yuen, R. K. K.; Song, L.; Lu, H. Synthesis, structure-property relationships of polyphosphoramides with high char residues. J. Mater. Chem. 2011, 21(18), 6621−6627.
21 Jiang, S.; Shi, Y.; Qian, X.; Xu, H.; Lo, S.; Gui, Z. Synthesis of a novel phosphorus- and nitrogen-containing acrylate and its performance as an intumescent flame retardant for epoxy acrylate. Ind. Eng. Chem. Res. 2013, 52(49), 17442−17450.
22 Tan, Y.; Shao, Z. B.; Chen, X. F.; Long, J. W.; Chen, L.; Wang, Y. Z. Novel multifunctional organic-inorganic hybrid curing agent with high flame-retardant efficiency for epoxy resin. ACS Appl. Mater. Interfaces 2015, 7(32), 17919−17928.
23 Tan, Y.; Shao, Z. B.; Yu, L. X.; Xu, Y. J.; Rao, W. H.; Chen, L.; Wang, Y. Z. Polyethyleneimine modified ammonium polyphosphate toward polyamine-hardener for epoxy resin: Thermal stability, flame retardancy and smoke suppression. Polym. Degrad. Stab. 2016, 131, 62−70.
24 Tan, Y.; Shao, Z. B.; Yu, L. X.; Long, J. W.; Qi, M.; Chen, L.; Wang, Y. Z. Piperazine-modified ammonium polyphosphate as monocomponent flame-retardant hardener for epoxy resin: flame retardance, curing behavior and mechanical property. Polym. Chem. 2016, 7(17), 3003−3012.
25 Li, C.; Kang, N. J.; Labrandero, S. D.; Wan, J.; González, C.; Wang, D. Y. Synergistic effect of carbon nanotube and polyethersulfone on flame retardancy of carbon fiber reinforced epoxy composites. Ind. Eng. Chem. Res. 2013, 53(3), 1040−1047.
26 Hu, S.; Song, L.; Pan, H.; Hu, Y.; Gong, X. Thermal properties

and combustion behaviors of flame retarded epoxy acrylate with a chitosan based flame retardant containing phosphorus and acrylate structure. J. Anal. Appl. Pyrolysis 2012, 97, 109−115.
27 Liu, X.; Gu, X.; Sun, J.; Zhang, S. Preparation and characterization of chitosan derivatives and their application as flame retardants in thermoplastic polyurethane. Carbohydr. Polym. 2017, 167, 356−363.
28 Chen, C.; Gu, X.; Jin, X.; Sun, J.; Zhang, S. The effect of chitosan on the flammability and thermal stability of polylactic acid/ammonium polyphosphate biocomposites. Carbohydr. Polym. 2017, 157, 1586−1593.
29 Yang, J. C.; Cao, Z. J.; Wang, Y. Z.; Schiraldi, D. A. Ammonium polyphosphate-based nanocoating for melamine foam towards high flame retardancy and anti-shrinkage in fire. Polymer 2015, 66, 86−93.
30 Deng, S. B.; Liao, W.; Yang, J. C.; Cao, Z.; Wang, Y. Z. Flame-retardant and smoke-suppressed silicone foams with chitosan-based nanocoatings. Ind. Eng. Chem. Res. 2016, 55(27), 7239−7248.
31 Amin, K. A. M.; Panhuis, M. I. H. Polyelectrolyte complex materials from chitosan and gellan gum. Carbohydr. Polym. 2011, 86(1), 352−358.
32 Sukhishvili, S. A.; Kharlampieva, E.; Izumrudov, V. Where polyelectrolyte multilayers and polyelectrolyte complexes meet. Macromolecules 2006, 39(26), 8873−8881.
33 Yang, J. C.; Liao, W.; Deng, S. B.; Cao, Z. J.; Wang, Y. Z. Flame retardation of cellulose-rich fabrics *via* a simplified layer-by-layer assembly. Carbohydr. Polym. 2016, 151, 434−440.
34 Shao, Z. B.; Deng, C.; Tan, Y.; Yu, L.; Chen, M. J.; Chen, L.; Wang, Y. Z. Ammonium polyphosphate chemically-modified with ethanolamine as an efficient intumescent flame retardant for polypropylene. J. Mater. Chem. A 2014, 2(34), 13955−13965.
35 Kong, Q. Q.; Liu, Z.; Gao, J. G.; Chen, C. M.; Zhang, Q.; Zhou, G.; Tao, Z. C.; Zhang, X. H.; Wang, M. Z.; Li, F. Hierarchical graphene-carbon fiber composite paper as a flexible lateral heat spreader. Adv. Funct. Mater. 2014, 24(27), 4222−4228.
36 Koester, K. J.; Ager Iii, J.; Ritchie, R. The true toughness of human cortical bone measured with realistically short cracks. Nat. Mater. 2008, 7(8), 672−677.
37 Ladani, R. B.; Ravindran, A. R.; Wu, S.; Pingkarawat, K.; Kinloch, A. J.; Mouritz, A. P.; Ritchie, R. O.; Wang, C. H. Multi-scale toughening of fibre composites using carbon nanofibres and z-pins. Compos. Sci. Technol. 2016, 131, 98−109.
38 Zhao, M.; Meng, L.; Ma, L.; Wu, G.; Xie, F.; Ma, L.; Wang, W.; Jiang, B.; Huang, Y. Stepwise growth of melamine-based dendrimers onto carbon fibers and the effects on interfacial properties of epoxy composites. Compos. Sci. Technol. 2017, 138, 144−150.
39 Wu, G.; Ma, L.; Liu, L.; Wang, Y.; Xie, F.; Zhong, Z.; Zhao, M.; Jiang, B.; Huang, Y. Interface enhancement of carbon fiber reinforced methylphenylsilicone resin composites modified with silanized carbon nanotubes. Mater. Design 2016, 89, 1343−1349.
40 Zhang, Z.; Yuan, L.; Liang, G.; Gu, A. A strategy and mechanism of fabricating flame retarding glass fiber fabric reinforced vinyl ester composites with simultaneously improved thermal stability, impact and interlaminar shear strengths. Polym. Degrad. Stab. 2016, 125, 49−58.
41 Zhao, F.; Huang, Y.; Liu, L.; Bai, Y.; Xu, L. Formation of a carbon fiber/polyhedral oligomeric silsesquioxane/carbon nanotube hybrid reinforcement and its effect on the interfacial properties of carbon fiber/epoxy composites. Carbon 2011, 49(8), 2624−2632.
42 González-Domínguez, J. M.; Ansón-Casaos, A.; Díez-Pascual, A. M.; Ashrafi, B.; Naffakh, M.; Backman, D.; Stadler, H.; Johnston, A.; Gómez, M.; Martinez, M. T. Solvent-free preparation of high-toughness epoxy-SWNT composite materials. ACS Appl. Mater. Interfaces 2011, 3(5), 1441−1450.
43 Lin, M. S.; Lee, S. T. Mechanical behaviours of fully and semi-interpenetrating polymer networks based on epoxy and acrylics. Polymer 1997, 38(1), 53−58.
44 Zhao, X.; Yang, L.; Martin, F. H.; Zhang, X. Q.; Wang, R.; Wang, D. Y. Influence of phenylphosphonate based flame retardant on epoxy/glass fiber reinforced composites (GRE): Flammability, mechanical and thermal stability properties. Compos. Part B- Eng. 2017, 110, 511−519.

https://doi.org/10.1007/s10118-018-2164-1